Differences between 1999 and 2010 across the Falkland Plateau: Fronts and water masses.

M. Dolores Pérez-Hernández (1,5), Alonso Hernández-Guerra (1), Isis Comas-Rodríguez (1), Verónica M. Benítez-Barrios (1), Eugenio Fraile-Nuez (2), Josep L. Pelegrí (3) and Alberto C. Naveira Garabato (4)

(1) Instituto de Oceanografía y Cambio Global (IOCAG), Universidad de Las Palmas de Gran Canaria (ULPGC), Las Palmas, Spain
(2) Centro Oceanográfico de Canarias, Instituto Español de Oceanografía, Santa Cruz de Tenerife, Spain
(3) Institut de Ciències del Mar, Consejo Superior de Investigaciones Científicas, Barcelona, Spain
(4) University of Southampton, National Oceanography Centre, Southampton, United Kingdom
(5) Department of Physical Oceanography, Woods Hole Oceanographic Institution, Woods Hole, USA

Abstract

Decadal differences in the Falkland Plateau are studied from the two unique full-depth hydrographic data collected during the ALBATROSS (April 1999) and MOC2-Austral (February 2010) cruises. Differences in the upper 100 dbar are due to changes in the seasonal thermocline, as the ALBATROSS cruise took place in the austral fall while the MOC-Austral in summer. The intermediate water masses seem to be very sensible to the wind conditions existing on their formation area, showing cooling and freshening for the decade as consequence of a higher Antarctic Intermediate Water (AAIW) contribution and of a decrease of the Subantarctic Mode Water (SAMW) stratum. The deeper layers do not exhibit any significant change in the water masses properties. The Subantarctic Front (SAF) in 1999 is observed at 52.2-54.8ºW with a relative mass transport of 32.6 Sv. In contrast, the SAF gets wider in 2010, stretching from 51.1 ºW to 57.2ºW (the Falkland Islands), and weakening to 17.9 Sv. Changes in the SAF can be linked with the westerly winds and are mainly affecting the northward flow of Subantarctic Surface Water (SASW), SAMW and AAIW/ Antarctic Surface Water

(AASW). The Polar Front (PF) carries 24.9 Sv in 1999 (49.8-44.4ºW), while in 2010 (49.9-49.2ºW) it narrows and strengthens to 37.3 Sv.

1. INTRODUCTION

The Antarctic Circumpolar Current (ACC) flows eastwards around the Antarctic continent, transporting roughly between 100 and 173 Sv (1 Sv $=10^6$ m^3 s^{-1} $\approx$ 10^9 kg s^{-1}, hereafter Sv will be the unit used) [Orsi *et al.*, 1995, Cunningham *et al*. 2003, Donohue *et al.* 2016]. Along its path, it connects the Atlantic, Pacific and Indian basins, exchanging heat and freshwater among other properties. Although convergence of net fluxes estimates have been achieved on basin scales [Ganachaud and Wunsch, 2003], the ACC flow into the Atlantic Ocean is critical to establish the magnitude and pathways of the Southern Ocean contribution to the deep global ocean ventilation.

Peterson and Whitworth [1989] suggested that the Subantarctic Front (SAF) and the Polar Front (PF), where the major velocity bands of the ACC occur, turn northwestward across the Falkland Plateau to the west of the Maurice Ewing Bank, along the Patagonian continental slope. This was supported by Peterson [1992], who estimated the large contribution of the ACC to the Falkland Current (60-70 Sv), revealing the importance of the overflow of southern waters to the South Atlantic boundary circulation. Peterson and Whitworth [1989] located the SAF near 53°W, as corroborated by Arhan *et al.* [2002], at a location where the ocean depth is 2000 m. Several studies have later examined the path of the PF around the Maurice Ewing Bank [Trathan *et al.*, 2000] and its branching around 49-50°W [Arhan *et al.*, 2002], with a possible meandering of the front according to Naveira Garabato *et al.* [2002].

The first hydrographic cruise along the Falkland Plateau was carried out in 1999. The ALBATROSS (Antarctic Large-scale Box Analysis and the Role of the Scotia Sea) cruise explored the ACC through the Drake Passage and the Scotia Sea (Figure 1). The

53 data of this cruise have been used to estimate relative transport, water masses, fluxes
54 and mixing across the Plateau [Naveira Garabato *et al*., 2003] and to provide a detailed
55 explanation of the deep waters in the Scotia Sea [Naveira Garabato *et al.*, 2002]. Later
56 on, this section has been compared with hydrographic cruises carried out north and
57 south of the Falkland Plateau to achieve a better knowledge of this area [Arhan *et al,*
58 2002; Smith *et al.*, 2010.]. However it is not until 2010 when this section is repeated.
59 In this study, the water masses, relative geostrophic velocities and transports across
60 an almost zonal hydrographic section carried out in 2010 along the Falkland Plateau are
61 evaluated. These data, together with the ALBATROSS cruise, are the only high-
62 resolution hydrographic data available on the region. Thus, results from the 2010 cruise
63 are compared with those obtained from the 1999 cruise in the same area [Naveira
64 Garabato *et al.*, 2003], with the objective of assessing possible relative transport and
65 water mass differences between the two surveys.
66 The paper is organized as follows. Section 'Data and Methods' presents the cruise,
67 data and methodology used in this study. Section 'Results' gives the description of the
68 different water masses existing on the study region, it shows the changes observed in
69 the θ/S isobaric surfaces, the location of the fronts, the results from Bindoff and
70 McDougall [1994] model and the changes in the relative geostrophic mass transport.
71 This paper concludes with a 'Discussion and conclusions' section that confronts our
72 estimations with the existing and provides with the concluding remarks of the research.
73
74 **2. DATA AND METHODS**
75 The MOC2-Austral cruise was carried out in February, 2010, on board the BIO
76 Hespérides. As shown in Figure 1a, 27 full-depth CTD stations were occupied across
77 the Falkland Plateau, tracking along the casts previously conducted in between 41ºW

78 and 57°W at the nominal latitude of 51°S during the ALBATROSS cruise in April 1999
79 [Naveira Garabato *et al.*, 2003]. With a spatial separation of 30 to 50 km, temperature
80 and salinity profiles were obtained using a SeaBird 911+ CTD with dual conductivity
81 and temperature sensors. The temperature sensor has an accuracy of 0.001ºC. The
82 conductivity sensors were calibrated on board with bottle sample salinities. To that end,
83 water samples were analyzed on a Guildline AUTOSAL 8400B salinometer with
84 accuracy better than 0.002 for single samples (salinity is expressed in the Practical
85 Salinity Scale).

86 Relative geostrophic velocities and mass transports are estimated for both the
87 ALBATROS and MOC-Austral cruises using the sea bottom as level of no-motion. The
88 water column is divided into 18 neutral density layers following the work of Naveira
89 Garabato et al. [2003] (see Table 1). Weddell Sea Deep Water (WSDW) is not found
90 along the Plateau, thus its density layers are not considered here.

91 Bindoff and McDougall [1994] describe a model to evaluate the temperature and
92 salinity variations in the water column. This model relates the temperature and salinity
93 in both pressure and density changes through the following equation:

$$\left.\frac{d\psi}{dt}\right|_z = \left.\frac{d\psi}{dt}\right|_{\gamma^n} - \left.\frac{dp}{dt}\right|_{\gamma^n} \frac{d\psi}{dp}$$

94 which shows that for a given property (ψ, temperature or salinity), the variations along
95 isobaric levels ($\left.\frac{d\psi}{dt}\right|_z$) can be described as the sum of changes along isoneutrals surfaces
96 ($\left.\frac{d\psi}{dt}\right|_{\gamma^n}$) and changes due to vertical displacements of the density surfaces, referred to as
97 heaving ($\left.\frac{dp}{dt}\right|_{\gamma^n} \frac{d\psi}{dp}$). This allows the comparison between the isobaric changes and the
98 sum of the two decomposed components, which represent the variations of the water
99 masses (warming and freshening) and the heaving. To apply this methodology,

100 temperature and salinity are interpolated onto a grid with a pressure interval of 20 dbar
101 (from 10 to 3500 dbar) and the following neutral density (kg m^{-3}) values: from 26 to
102 27.6 each 0.02, from 27.7 to 28 each 0.01 and from 28.005 to 28.5 each 0.005. This
103 vector is selected to properly represent the different structures found in the water
104 column.

105 In addition, Sea surface height (SSH) was downloaded from AVISO
106 (http://www.aviso.oceanobs.com/). Data between February 10 and 20, 2010 are used for
107 the analysis of the MOC-Austral cruise results. Data of February and April from 1993
108 to 2016 are used to estimate the average seasonal geostrophic transport in each month.
109

110 **3. RESULTS**

111 **3.1 Water Masses**

112 Water masses in the study region are labeled following Naveira Garabato *et al.*
113 [2003]. The isoneutrals 26.90, 27.20, 27.60 and 28.00 kg m^{-3} (red solid lines in Figure
114 1b) divide the water column into Subantarctic Surface Water (SASW), Subantarctic
115 Mode Water (SAMW), Antarctic Intermediate Water (AAIW) mixed with Antarctic
116 Surface Water (AASW), Upper Circumpolar Deep Water (UCDW) and Lower
117 Circumpolar Deep Water (LCDW), respectively.

118 Figure 2 shows that, in both cruises, the Circumpolar Deep Water (CDW) is the
119 most homogenous water mass. The UCDW in the ALBATROSS cruise presents a wider
120 temperature range and it is less homogeneous than in the MOC-Austral cruise. Figure 2
121 also exhibits that the stratums of AAIW+AASW and SAMW are quite different
122 between cruises. The AAIW+AASW stratum of the MOC-Austral cruise presents a
123 minimum that consists on temperatures below 1.2ºC and salinities around 34. This
124 minimum indicates that the contribution of AAIW is higher in 2010 than in 1999. In

125 contrast, in the same stratum, the ALBATROSS cruise shows a thicker layer of AASW.
126 The SASW in 1999 reaches higher salinities and temperatures than in the MOC-Austral
127 cruise (this can be better observed in Figure 1b grey dots). It is also worth mentioning
128 the existing difference between the SAWM stratums of both cruises, as the one of the
129 ALBATROSS cruise has a wider range of salinities than the one of the MOC-Austral
130 (Figure 2). The upper layers are less comparable as the cruises took place in different
131 seasons, which implies different precipitation/evaporation and winds that will directly
132 affect the SASW stratum.
133
134 **3.2 Fronts**
135 In Figure 3, the prominent slope of the γ^n-surfaces together with the intensified
136 relative velocities, point out the presence of the SAF and PF near their historically
137 reported locations [Orsi *et al.*, 1995]. In 1999, a northward-flowing jet accompanies the
138 SAF, extending the front's influence from the surface down to approximately 1500 m
139 between 52.2 and 54.8°W (Figure 3a, stations 160 to 165). In contrast, the SAF is
140 displaced to the west in 2010, extending from the Falkland shore (57.2ºW) to 51.1ºW
141 (stations 5 to 17) and the horizontal density gradient and associated relative geostrophic
142 velocities are weaker (Figure 3b). Regarding the PF, its quasi-barotropic presence and
143 effect on the water column is most noticeable in 2010 (Figure 3b, stations 20 and 21),
144 when it intensifies, displaying the strongest flow to the north around 49.5°W. Figure 3a
145 shows how this front is weaker in 1999, when it extends approximately in between 44.4
146 and 49.8°W and no intense jets are triggered by its presence (stations 146 to 156).
147 It can be observed how these fronts are revealed by the slopping isoneutrals,
148 suffering significant changes between the two oceanographic cruises. Therefore, it is

149 important to determine which variations in potential temperature and salinity are due to
150 water masses changes and which are caused by the displacement of the γ^n-surfaces.
151
152 **3.3 The θ/S Isobaric Changes**
153 Figure 4 reveals that in the decade, the waters shallower than 50 dbar (roughly the
154 SASW stratum) exhibit a significant increase of temperature and salinity, being of 0.5ºC
155 and 0.12, respectively (Figure 4a to d). This surface increase is probably caused by the
156 fact that the area was sampled in very different seasons: while the MOC-Austral cruise
157 took place in the austral summer, the ALBATROSS cruise was carried out during the
158 austral fall.
159 In the waters immediately beneath (from 50 dbar to 500 dbar), the intermediate
160 stratums of SAMW and AAIW+AASW present a decrease of temperature of 0.8ºC and
161 0.4ºC, respectively (Figure 4a and b). In contrast, while salinity for the AAIW+AASW
162 stratum also decreases 0.01, the salinity of the SAMW increases 0.02 (Figure 4c and d).
163 In these intermediate stratums, at roughly the location of the fronts (between stations 5-
164 17 and 20-21), a remarkable decrease in temperature can be seen (Figure 4a). In
165 between stations 9-12, where the SAF stands, the UCDW exhibits a remarkable increase
166 in salinity. This increase gets compensated in the average with the decrease observed
167 throughout the stratum. The same is observed in the area of the PF, where an increase of
168 salinity is registered at the UCDW and AAIW/AASW stratums (Figure 4 c).
169 The UCDW and LCDW do not show any significant changes in temperature. The
170 UCDW increases 0.01 in salinity while the LDCW doesn't show any significant
171 difference in salinity (Figure 4c and d).
172
173 **3.4 Results of applying the Bindoff and McDougal [1994] analysis**

The temperature and salinity isobaric changes, their decomposition and the sum of the two components are plotted in Figures 5a and 5b, respectively. Except for certain depth ranges, the sum of the components (grey line) compares reasonably well with the isobaric change (black line, θ_z and S_z) indicating that the decomposition has been successfully performed. The few discrepancies observed will be analyzed at the end of the section.

The surface and intermediate temperature and salinity variations are affected by both mechanisms; changes along neutral surfaces (θ_n and S_n, blue lines) and changes due to vertical displacement of the isoneutrals ($-N\theta_z$ and $-NS_z$, red lines) (Figure 5a and b). In the SASW stratum (pressure<100 dbar) an increase of 0.7ºC in temperature and 0.1 in salinity per decade is observed in Figure 5a and b, respectively. This increase can also be observable in Figure 5c. These increases come together with a temperature-driven vertical displacement of the isoneutrals (Figure 5a red line). As the cruises took place on different seasons the most plausible explanation for this shoaling is the different depths of the seasonal thermocline, being shallower in summer (2010) than in fall (1999).

In contrast with the upper layer, the SAMW and AAIW/AASW stratums present a decadal decrease of temperature (-0.6ºC) and salinity (-0.07) in between 100 dbar and 500 dbar (Figure 5a and b). These changes can also be observed in the average θ/S-diagram for the AAIW/AASW (Figure 5c). The SAMW and AAIW/ASW stratums occupy the same depth range, but the AAIW/ASW water mass spans over a higher area (Fig 3). Hence, the decomposition shown in Figure 5a and b is mainly showing the behavior of the AAIW/AASW stratum and, therefore, it does not match with the increase in salinity observed in Figure 5c for SAMW. On Figure 5c the lines linking points of equal pressure for the SAMW and AAIW/AASW stratums are not parallel to the isopycnals, indicating as well, displacement of the isoneutrals surfaces. This

displacement is a deepening of the isoneutrals, mainly driven by the salinity. At the level of the UCDW no changes are observed (Figure 5 a to c). In contrast, the LCDW stratum shows a deepening of the isoneutrals driven by both temperature and salinity, although no changes along neutral surfaces is observed (Figure 5 a to c).

As seen in Figure 5, the sum of the components compares reasonably well to the isobaric changes. However, a careful inspection reveals some discrepancies, which take place between 52 and 57ºW and around 49.5ºW. These are the approximate locations of the SAF and PF fronts. These gradients cause the vertical displacement of more than 200 dbar for some isoneutrals, invalidating at these specific locations, the linear expansion used to derive the proposed decomposition model, as was also found in the Gulf Stream by Arbic and Owens [2001]. Thus, in Figure 6 a sensitivity analysis is carried out by using the model of Bindoff and McDougall [1994] without the stations involved in the fronts, taking into account only the stations 18 (157) and 28 to 31 (145 to 142) for the 2010 (1999) survey. For the surface SASW water mass, the same behavior is found with or without fronts: an increase of temperature and salinity, though slightly higher in the decomposition done without the fronts (0.9ºC and 0.15 *vs.* 0.7ºC and 0.1), and a temperature-driven shoaling of the isopycnals. Likewise, in the range 100-500dbar, where the SAMW and AAIW/AASW stratums appear, the decomposition shows the same pattern; a slightly smaller decrease in temperature (-0.4ºC) and salinity (-0.04) again accompanied with a salinity-driven deepening of the isopycnals.

In contrast, from 500 dbar to the bottom two differences appear between both decompositions. The first one occurs in between 500 dbar and 2000 dbar, in both decompositions a slightly increase of temperature and salinity is observed but in the one carried out without the fronts it appears with a salinity-driven shoaling of the isopycnals. This depth range is mainly occupied by the UCDW stratum. The second

224 significant change between both decompositions appears at the bottom of the profile, at
225 the domain of the LCDW. As the stations east of the MOC-Austral station 28
226 (ALBATROSS station 148) are shallower than 2400 dbar, this decomposition is mainly
227 showing the changes suffered at stations 18. This station is located between both fronts,
228 and shows a temperature-driven deepening of the isopycnals. The result of this stratum
229 can be neglected, as one station cannot be considered statistically significant to provide
230 representative results.
231
232 **3.5 Relative Geostrophic Transport changes**
233 Some significant differences are observed in the relative mass transport estimates
234 for 1999 and 2010 across the hydrographic line along the Falkland Plateau (Table 1).
235 The accumulated transports evidence the important role played by the SAF and PF on
236 the relative mass transport across the section during both realizations (Figure 7). During
237 the MOC-Austral cruise the SAF-associated jet is displaced westward and weakens 14.7
238 Sv as compared with the ALBATROSS observations (Figure 4 and table 1). This affects
239 the relative transport of all stratums except LCDW. In contrast, the location of the PF
240 remains unchanged between both cruises but it strengthens up to 37.3 Sv during the
241 MOC-Austral cruise (*vs.* the 24.9 Sv registered in the ALBATROSS survey), affecting
242 the relative transports of all water strata. In 2010, immediately east of the PF, at
243 47.8ºW, a countercurrent appears carrying -8.8 Sv to the south. Figure 8 shows the
244 average SSH for the 2010 MOC-Austral cruise with the aim to understand the source of
245 this counter-flow. In this Figure, the PF flows to the north around station 20 and
246 partially diverting southward at station 23. This meandering of the PF has already been
247 reported in previous studies [Naveira Garabato *et al.*, 2002].

248 The relative net transport during the MOC-Austral cruise is 9.2 Sv weaker than in
249 the ALBATROSS cruise as an outcome of a more intense SAF. SASW, AAIW/AASW
250 and UCDW present lower values in 2010 than in 1999, being the surface and
251 intermediate stratums the ones with the highest decadal transport differences (Figure 7
252 and table 1). This is presumably due to a weaker SAF in 2010 (17.9 Sv) than in 1999
253 (32.6 Sv) (Table 1). The LDCW stratum does not registers the SAF due to the
254 bathymetry. Thus, the only northward contribution to this stratum is done by the PF,
255 which is stronger in 2010 than in 1999 from the SAMW stratum to the bottom. The total
256 transports of the PF are 37.3 Sv in 2010*vs.* 24.9 Sv in 1999.
257 Figure 9 exhibits the vertical structure of the calculated mass transport in the
258 different layers, which define each water mass. The geostrophic transports in
259 ALBATROSS (1999) and MOC Austral (2010) hydrographic cruises behave likewise
260 across the water column. The transports from the surface to the UCDW stratums are
261 affected by a noticeable northward net transport decrease of 10.6 Sv from 1999 to 2010.
262 In contrast, the LCDW exhibits an increase of 1.4 Sv of the northward flow in 1999 and
263 2010.
264 To put all the estimated transports in context, the monthly 1993-2016 averaged
265 geostrophic velocities from AVISO are interpolated to the station pairs of both cruises
266 and integrated by using the stations distance and the average depth of the SASW
267 stratum (50 m). This is shown in Figure 10, where the 1993-2016 average of all
268 Februaries (Aprils) is contrasted with the estimated relative transport of the MOC
269 Austral (ALBATROS) upper stratum. It is seen that there is no climatological
270 significant difference between the estimations of both months. Hence, the positions and
271 transports (expressed as mean ± standard deviation) of the SAF and PF in the AVISO
272 derived transports are 2.5±0.5 Sv at the longitudinal range 52.97-56.96ºW and 1.1±0.7

Sv at 47.49-51.34ºW, respectively. The SAF AVISO estimated transport is approximately the average between the SASW transports of the ALBATROSS (3.2 Sv) and MOC Austral (1.9 Sv). The PF observed in the AVISO data covers a wider range of longitudes than those of the hydrographic surveys. Its transport is slightly smaller than for the ALBATROSS cruise (2.0 Sv) and non-significantly different from the MOC Austral (1.6 Sv) at the SASW stratum (Table 1).

4. DISCUSSION AND CONCLUSIONS

The decadal differences in the Falkland Plateau are studied from full-depth hydrographic data collected during the ALBATROSS (April 1999) and MOC2-Austral (February 2010) cruises. Water mass changes are explored in terms of changes along neutral surfaces and changes due to vertical displacements of γ^n-surfaces, applying the model proposed by Bindoff and McDougall [1994]. Variability in the SAF and PF location and mass transport is inferred from relative geostrophic velocities estimated by using the sea-bottom as the level of no-motion.

The SASW stratum presents a wider range of salinities and temperatures in 1999 than in 2010 as shown in the θ/S diagram. In spite of this, the θ/S isobaric changes show an increase of surface temperatures and salinities matching the Bindoff and McDougall [1994] model's result for changes along neutral surfaces. The model also exhibits shoaling of the isopycnals. The most plausible source for these differences is the fact that the hydrographic cruises took place in different seasons (ALBATROSS in austral fall and MOC-Austral in austral summer). Hence the seasonal thermocline has probably changed its depth due to the different seasonal heating and precipitation. The scarce in situ observations in the area do not allow any further conclusion.

297 SAMW expands over a higher depth range and presents a wider range of salinities
298 in 1999 than in 2010 (Figures 2 and 4). In contrast, the θ/S diagram and isobaric
299 changes for the AAIW/AASW stratum show a decrease in temperature and salinity in
300 2010 when the AAIW/AASW occupies a higher depth range (Figures 2 and 4). As both
301 Bindoff and McDougall [1994] model estimations (with and without frontal zones)
302 agree in that the changes in the intermediate stratums are due to the displacement of γ^n-
303 surfaces, some changes are likely to have occurred between 1999 and 2010 in the
304 Falkland Plateau. The Bindoff and McDougall [1994] model reveals a deepening of the
305 isoneutrals at these levels, where the AAIW/AASW stratum occupies a higher depth
306 range than SAMW. An explanation for changes in those stratums can be found in
307 Naveira Garabato *et al*. [2009]. Figure 10a shows the mean wind stress of the winters in
308 the period 1998 - 2010. This figure is analogous to Figure 10a of Naveira Garabato *et*
309 *al*. [2009]. In the climatological mean a continuous wind stress magnitude spreads west
310 from South America (Figure 10a). Figures 10b and 10c exhibits the previous winter
311 anomalies to the ALBATROSS and MOC-Austral cruises, respectively. These
312 anomalies look very different between themselves. Figure 10b shows a large eastward
313 (positive) wind stress anomaly in the Southern Pacific. Naveira Garabato *et al*. [2009]
314 suggest that this structure causes a shift in the SAMW formation area. This matches
315 with the changes observed in Figures 2 and 4, where the SAMW stratum area is
316 reduced. It also agrees with the isobaric changes reported, a decrease in temperature of
317 0.8ºC and an increase in salinity of 0.02 from 1999 to 2010.
318 Naveira Garabato *et al*. [2009] also reported that the 1998-wind stress anomaly
319 pattern shown in Figure 10b generates a shutdown of the AAIW formation. Due to this,
320 a minimum of temperatures (<1.2ºC) and salinities (ca. 34) can be observed only for the
321 MOC-Austral cruise in Figures 1b and 2b. The shutdown of the AAIW formation in

322 1998 is responsible of the observed changes from 1999 to 2010 at this stratum. Across
323 the decade, the AAIW/AASW stratum increases the spanning area at intermediate
324 layers and suffers a decrease of 0.6ºC in temperature and of 0.07 in salinity, which is
325 accompanied with a deepening of the isoneutrals. Wind-driven changes in the ACC
326 isobaric surfaces were also observed in Böning et al [2008], where a deepening of the
327 isopycnals 27.2 and 27.4 kg m^{-3} is described. The reported decrease of 0.07 in salinity
328 agrees with the decadal trend of the ACC at 300-500 dbar observed in Böning et al.
329 [2008] shown in their Figure 4. In contrast, they find an increase of temperature at the
330 same layer, probably due to the contribution of other intermediate waters into the ACC.
331 The SAF and PF undergo some displacements and variations in intensity between
332 1999 and 2010. The SAF in 1999 is observed at 52.2-54.8ºW with a relative mass
333 transport of 32.6 Sv and, while it is wider in 2010, reaching the Falkland Islands, it
334 weakens to roughly half of the transport (17.9 Sv). The SAF is the main path for the
335 northward flow of SASW, SAMW and AAIW/AASW into the Atlantic Basin. The PF
336 also contributes to this northward flow, being important for the UCDW and LCDW.
337 The PF in 1999 is located in the longitudinal range 49.8-44.4ºW carrying 24.9 Sv, while
338 in 2010 it narrows, centering on 49.9-49ºW and strengthening to 37.3 Sv. The PF in
339 2010 carries the highest relative northward transport of the study area, but nearly 8 Sv
340 of it recirculate back southward as seen in the SSH image. This meandering of the PF
341 was also observed in Naveira Garabato *et al.*, [2002]. The average of the AVISO
342 climatological seasonal transport is non-significantly different between February and
343 April. Thus, the observed changes in transport are due to interannual variability.
344 The abrupt decrease of the SAF to almost half of its transport between both decades has it
345 source on the different wind patterns observed in Figure 10 and described in Naveira Garabato
346 et al. (2009). The changes on these westerly winds that circles Antarctica are driven by the
347 southern annular mode (SAM). Combes et al. (2014) analyses the 1990 to 2012 trend of the

SAM and its relation with the Falkland Current (which nourishes from the SAF). On their study they report a decrease on the Drake Passage transports and of the Falkland Current after 1999-2000 as consequence of a weakening of the westerly winds.

To conclude, a seasonal change of the thermocline is observed in the surface layer. Changes in the westerly winds driven by the increasing trend of the SAM (Combes et al. 2014 and Naveira Garabato et al. 2009) have an important effect on the water masses and transports observable in the Falkland Plateau. The intermediate water masses of the study area seem to be very sensible to the wind conditions existing on their formation area. Hence in 2010 an increase (decrease) of the AAIW/AASW (SAMW) stratum is observed together with a cooling, freshening and deepening of the isopycnals at this level. The CDW layers do not exhibit any significant change in the water masses properties, being the most homogenous water mass. However the LCDW exhibited a temperature and salinity driven deepening of the isopycnals from 1999 to 2010. The net transport is 9.2 Sv weaker in 2010 than in 1999 and is mainly explained by a decrease on the transport of the SAF. Fronts change their width and strength between cruises, being the SAF/PF in 2010 wider/thinner and weaker/stronger than in 1999. Changes on the water masses, position and transport contribution of the SAF and PF to the north directly affect the Brazil-Malvinas Confluence zone, which moves to the south when the SAF weakens (Combes et al. 2014). This strong frontal zone is critical for the southern hemisphere meridional overturning, is where the deep western boundary separates from the Argentinian basin and is a high energy area that contributes to the active water masses transformation (Mason et al. 2017).

Acknowledgments

This study has been performed thanks to the MOC2 (CTM2008-06438-C02-02/MAR) and Sevacan (CTM2013-48695), financed by the Spanish Government. The ALBATROSS cruise was funded by a Natural Environment Research Council grant (GR3/11654). This work was completed while M.D. Pérez-Hernández was a Ph.D. student in the IOCAG Doctoral Programme in Oceanography and Global Change. The authors would like to thank David Sosa, Rayco Alvarado and, all the scientific team and crew on board the BIO Hespérides for their hard work at sea during the MOC-Austral cruise.

382 **References**

383 Arbic, B. K., and W. B. Owens (2001), Climatic warming of Atlantic intermediate
384 waters, J. Climate, 14 (20), 4091–4108.
385
386 Arhan, M., Naveira Garabato A.C., Heywood, K.J., Stevens, D.P., (2002.) The
387 Antarctic Circumpolar Current between the Falkland Islands and South Georgia. J.
388 Phys. Oceanogr. 32 (6), 1914–1931, doi: 10.1175/1520-0485
389
390 Bindoff, N. L., and T. J. McDougall (1994), Diagnosing climate change and ocean
391 ventilation using hydrographic data, J. Phys. Oceanogr., 24 (6), 1137–1152.
392
393 Böning, C.W., Dispert, A., Visbeck, M., Rintoul, S. R. And Schwarzopf, U. (2008), The
394 response of the Antarctic Circumpolar Current to recent climate change, Nature
395 Geoscience, 1, 864-869, doi:10.1038/ngeo362
396
397 Comas-Rodríguez, I., Hernández-Guerra, A., McDonagh, E., 2011. Referencing
398 geostrophic velocities using ADCP data at 24.5°N (North Atlantic). Sci. Mar. 74 (2),
399 331–338, doi: 10.3989/scimar.2010.74n2331
400
401 Combes, V., and R. P. Matano (2014), Trends in the Brazil/Malvinas Confluence
402 region, Geophys. Res. Lett., 41, 8971–8977, doi:10.1002/2014GL062523.
403 Cunningham S.A., Alderson S.G., King, B.A., Brandon M.A., 2003. Transport
404 variability of the Antarctic Circumpolar Current in Drake Passage. J. Geosphys. Res.
405 Oceans. 108 (C5), doi: 10.1029/2001JC001147
406

Dibarboure, G., O. Lauret, and F. Mertz, 2015. SSALTO/ DUACS User Handbook: (M) SLA and (M) ADT Near-Real Time and Delayed Time Products. AVISO Rep. CLS-DOS- NT 06-034, Issue 4.4. SALP-MU-P-EA-21065-CLS.

Donohue, K. A., K. L. Tracey, D. R. Watts, M. P. Chidichimo, and T. K. Chereskin (2016), Mean Antarctic Circumpolar Current transport measured in Drake Passage, Geophys. Res. Lett., 43, 11,760–11,767, doi:10.1002/2016GL070319.

Egbert, G., Bennett, A., Foreman, M., 1994. TOPEX/POSEIDON tides estimated using a global inverse model. J. Geophys. Res. 99 (C12), 24821, doi: 10.1029/94JC01894

Egbert, G., Erofeeva, S., 2002. Efficient inverse modeling of barotropic ocean tides. J. Atmos. Ocean. Tech. 19 (2), 183–204, doi: 10.1175/1520-0426

Fischer, J., Visbeck, M., 1993. Deep velocity profiling with self-contained ADCPs. J. Atmos. Ocean. Tech. 10 (5), 764–773, doi: 10.1175/1520-0426

Ganachaud, A., Wunsch, C., 2003. Large-Scale Ocean Heat and Freshwater Transports during the World Ocean Circulation Experiment. J. Climate 16 (4), 696–705, doi: 10.1175/1520-0442

Mason, E., Pascual, A., Gaube, P., Ruiz, S., Pelegrí, J. L. and Delepoulle, A. (2017), Subregional characterization of mesoscale eddies across the Brazil-Malvinas Confluence. J. Geophys. Res. Oceans. Accepted Author Manuscript. doi:10.1002/2016JC012611

Naveira Garabato A.C., Heywood, K.J., Stevens, D.P., 2002. Modification and pathways of Southern Ocean Deep Waters in the Scotia Sea. Deep-Sea Res. I 49 (4), 681–705, doi: 10.1016/S0967-0637(01)00071-1

Naveira Garabato, A.C., Stevens, D.P., Heywood, K.J., 2003. Water Mass Conversion, Fluxes, and Mixing in the Scotia Sea Diagnosed by an Inverse Model. J. Phys. Oceanogr. 33 (12), 2565–2587, doi: 10.1175/1520-0485

Naveira Garabato, A.C., Jullion, L., Stevens, D.P., Heywood, K.J., King, B.A.,2009. Variability of Subantartic Mode Water and Antarctic Intermediate Water in the Drake Passage during the Late-Twentieth and Early-Twenty-First Centuries. J. of Clim. 22, 3661-3688, doi: 10.1175/2009JCLI2621.1

Orsi, A.H., Whitworth III, T., Nowlin Jr., W.D., 1995. On the meridional extent and fronts of the Antarctic Circumpolar Current. Deep-Sea Res. I 42 (5), 641–673, doi: 10.1016/0967-0637

Peterson, R.G., Whitworth III, T., 1989. The subantarctic and polar fronts in relation to deep water masses through the southwestern Atlantic. J. Geophys. Res. 94 (C8), 10817–10838, doi: 10.1029/JC094

Peterson, R.G., 1992. The boundary currents in the western Argentine Basin. Deep-Sea Res. A 39 (3-4), 623–644, doi: 10.1016/0198-0149

457 Smith, I.J., Stevens, D..P., Heywood, K. J., Meredith, M. P., 2010. The flow of the
458 Antarctic Circumploar Current over the North Scotia Ridge. Deep-Sea Res. I. 56, 14-28.
459 doi:10.1016/j.dsr.2009.10.010
460
461 Trathan, P.N., Brandon, M.A., Murphy, E.J., Thorpe, S.E., 2000. Transport and
462 structure within the Antarctic Circumpolar Current to the north of South Georgia.
463 Geophys. Res. Lett. 27 (12), 1727–1730, doi: 10.1029/1999
464
465 Whitworth III, T., Nowlin, W.D., Worley, S.J., 1982. The Net Transport of the
466 Antarctic Circumpolar Current through Drake Passage. J. Phys. Oceanogr. 12 (9), 960–
467 971, doi: 10.1175/1520-0485
468
469

Tables:

Table 1. SAF, PF and net geostrophic mass transport (Sv) per cruise and water mass. The last row shows the net transport, while the last column indicates the transport difference between cruises.

	ALBATROSS (1999)			**MOC-Austral (2010)**			**Difference (2010-1999)**		
	SAF	**PF**	**Net**	**SAF**	**PF**	**Net**	**SAF**	**PF**	**Net**
SASW γ^n<26.80	3.2	2.0	4.5	1.9	1.6	2.3	-1.3	-0.4	-2.2
SAMW 26.80<γ^n<27.10	5.1	1.0	4.9	1.4	1.8	2.2	-2.9	0.8	-2.7
AAIW / AASW 27.10<γ^n<27.50	15.5	8.3	16.8	10.9	9.7	11.8	-4.6	1.4	-5.0
UCDW 27.50<γ^n<27.90	8.6	12.0	12.4	3.8	20.1	11.7	-4.8	8.1	-0.7
LCDW 27.90<γ^n	0.1	1.6	0.3	0.0	4.1	1.7	-0.1	2.5	1.4
Net	32.6	24.9	38.9	17.9	37.3	29.7	-14.7	12.4	-9.2

List of Figures

4 Vertical sections of differences in (a) potential temperature and (c) salinity in isobaric levels, for the decade 1999 to 2010 The lines superimposed over the vertical sections (grey lines for the 1999 section and black lines for the 2010 section) stand for the isoneutrals defining the different water masses in the region (26.90, 27.20, 27.60 and 28.00 $\mathrm{kg\,m^{-3}}$). MOC-Austral station numbering and the fronts (SAF (gray1999, black 2010) and PF) location are displayed on top axis. Side panels show the zonally averaged differences of temperature (b) and salinity (d), respectively (solid black lines) together with their 95% confidence interval based on a Students t-test (dashed grey lines). 8

5 Isobaric changes from 1999 to 2010 (θ_z, black line) decomposed into changes along neutral surfaces (θ_n, S_n,blue line) and changes due to the vertical displacement of isoneutrals (-Nθ_z, -NS_z red line) for (a) potential temperature and (b) salinity. The grey line shows the sum of both components. The lower panel (c) shows the average profile of θ/S for each cruise together with the densities that divide the water column into the different water masses (26.90, 27.20, 27.60 and 28.00 $\mathrm{kg\,m^{-3}}$; red lines) and the link in between points of equal pressure (dashed blue lines). 9

6 Comparison between the isobaric changes from 1999 to 2010 carried out with the whole dataset of each year (a and b, same as Fig 5) and without the stations were the fronts are located (c and d). Isobaric changes from 1999 to 2010 (θ_z, black line) decomposed into changes along neutral surfaces (θ_n, Sn,blue line) and changes due to the vertical displacement of isoneutrals (-Nθ_z, -NS$_z$ red line) for temperature (a and c) and Salinity (b and d). The grey line shows the sum of both components.

7 West to east accumulated relative geostrophic mass transport, computed across the ALBATROSS and MOC-Austral hydrographic sections. Station numbering and the fronts (SAF and PF) location are displayed on top axis. Note the different vertical scales.

8 AVISO Sea Surface Height (SSH) for the MOC-Austral cruise. Isolines have a separation of 5 cm.

9 Relative geostrophic mass transport per layer across the ALBATROSS and MOC-Austral sections.

10 West to East accumulated relative geostrophic mass transport from AVISO averaged from 1993 to 2016, together with their standard deviations: April (grey solid line) and February (black solid line). For this calculation, the depth of 50 m has been considered to compute the mass transport that corresponds to the SASW stratum. Dashed lines are the west to east accumulated relative geostrophic mass transports shown in Figure 7 for the SASW for the ALBATROS (grey) and MOC Austral (black) carried out in April and February, respectively.

11 Maps of NCEP-NCAR a) winter (July-September) mean wind stress in Pa (arrows, color indicates magnitude) for the time period 1998-2010. b) Winter wind stress anomaly (Pa) for year 1998. c) Same as b) but for 2009. 15

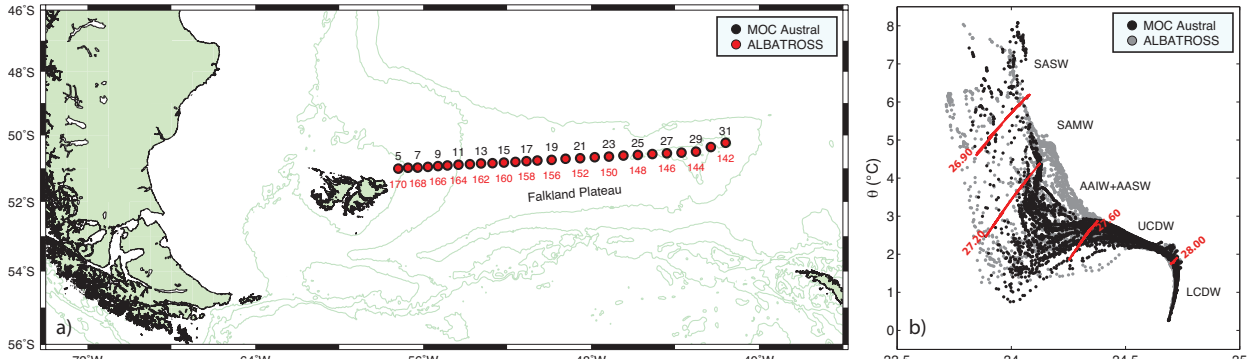

FIG. 1. a) Hydrographic stations across the Falkland Plateau carried out during ALBATROSS (1999, red station numbers) and MOC-Austral (2010, station numbers) cruises. b) θ-S diagram for both cruises. Red solid lines represent the γ^n values (26.90, 27.20, 27.60 and 28.00 kg m^{-3}) defining the different water masses in the region.

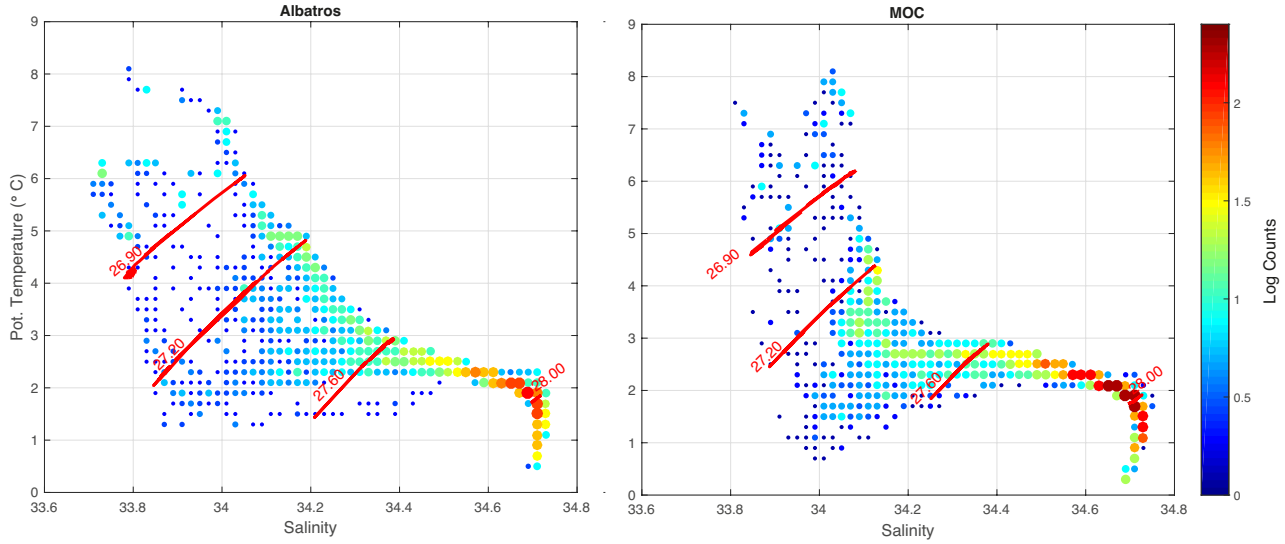

FIG. 2. A volumetric potential temperature-salinity diagram for the a) ALBATROSS and b) MOC-Austral cruises. Red solid lines represent the γ^n values (26.90, 27.20, 27.60 and 28.00 $\mathrm{kg\,m^{-3}}$) defining the different water masses in the region. Dot size and color indicates the logarithm of counts.

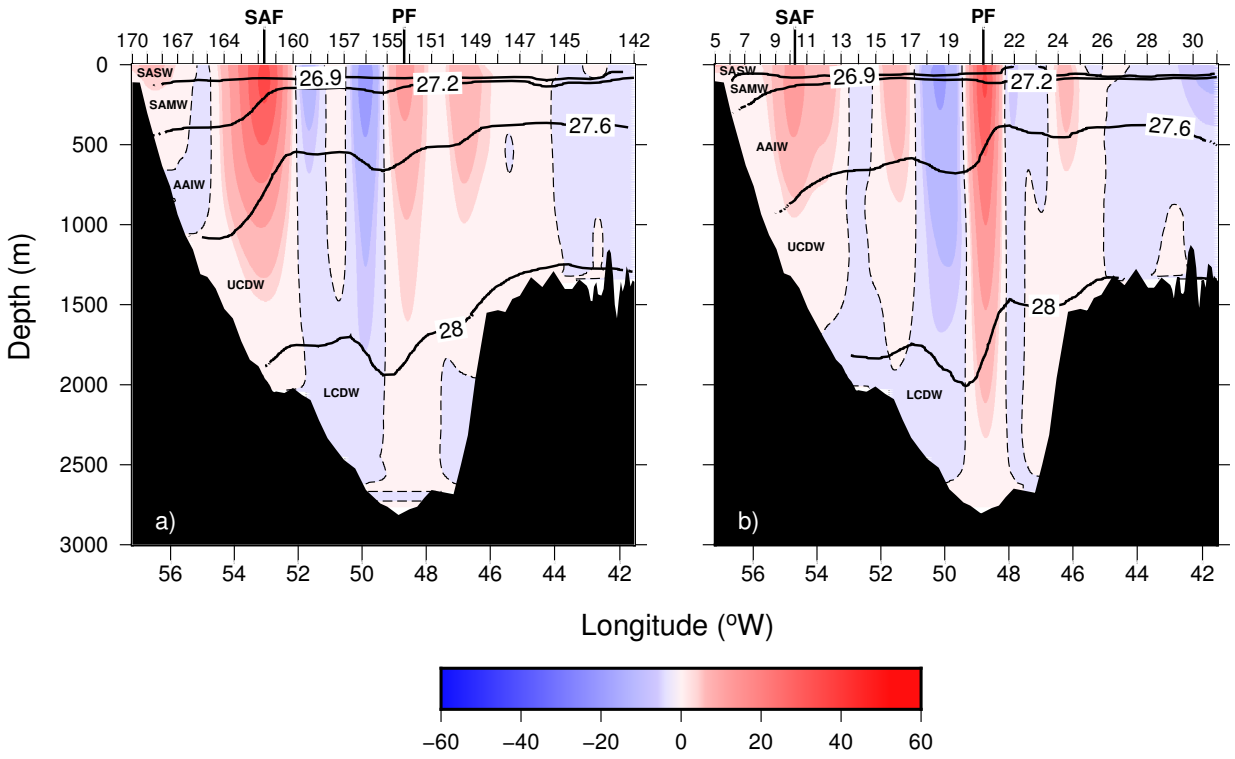

FIG. 3. Geostrophic velocity (cm/s, positive northward) relative to the bottom for a) the ALBATROSS cruise and b) the MOC-Austral cruise. Black dashed lines mark zero cm/s velocities. Thick black lines stand for the representative isoneutrals (26.90, 27.20, 27.60 and 28.00 $\mathrm{kg\,m^{-3}}$) defining the water masses in the region. Station numbering and the fronts (SAF and PF) location are displayed on top axis.

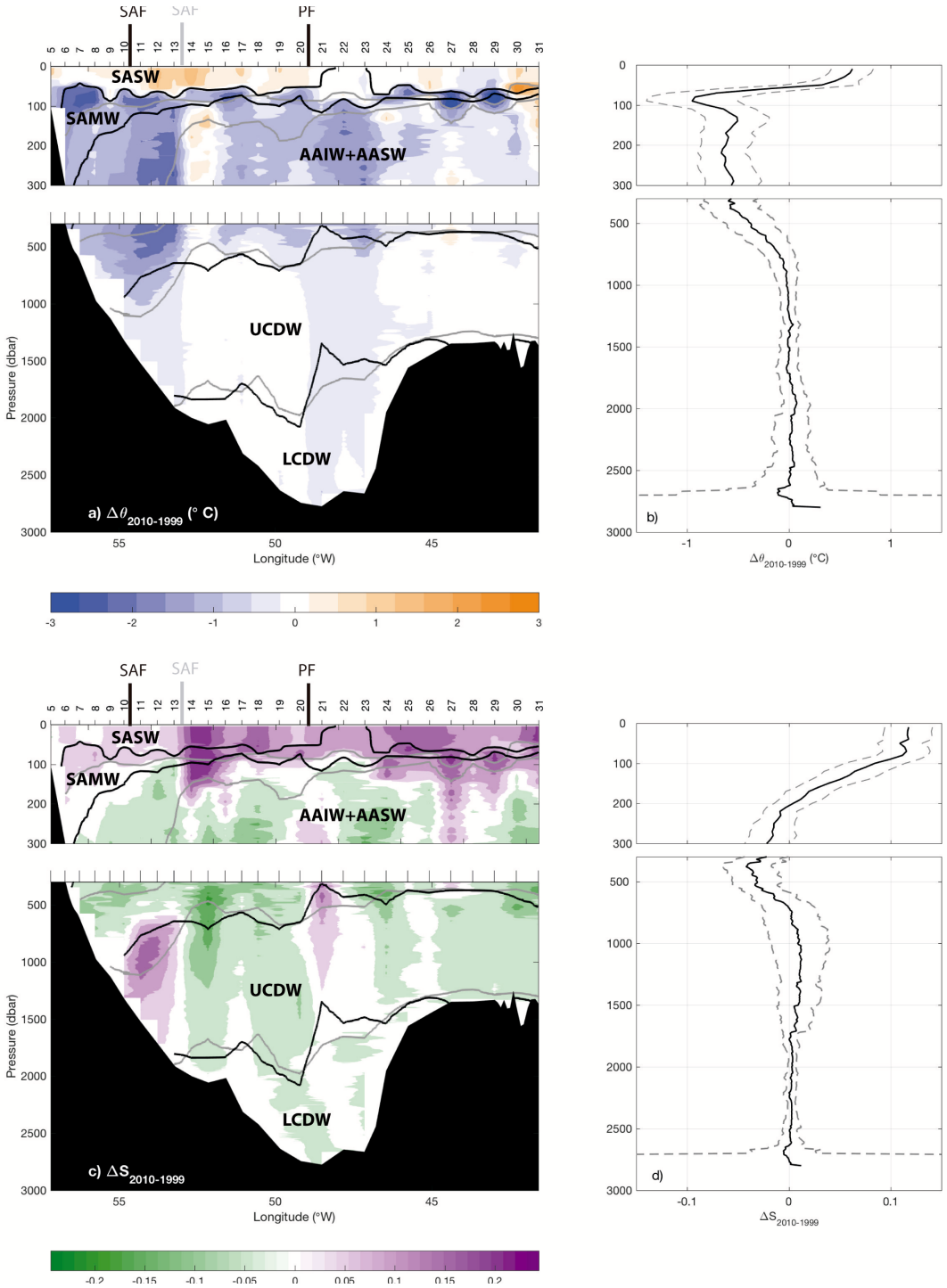

FIG. 4. Vertical sections of differences in (a) potential temperature and (c) salinity in isobaric levels, for the decade 1999 to 2010 The lines superimposed over the vertical sections (grey lines for the 1999 section and black lines for the 2010 section) stand for the isoneutrals defining the different water masses in the region (26.90, 27.20, 27.60 and 28.00 kg m^{-3}). MOC-Austral station numbering and the fronts (SAF (gray1999, black 2010) and PF) location are displayed on top axis. Side panels show the zonally averaged differences of temperature (b) and salinity (d), respectively (solid black lines) together with their 95% confidence interval based on a Students t-test (dashed grey lines).

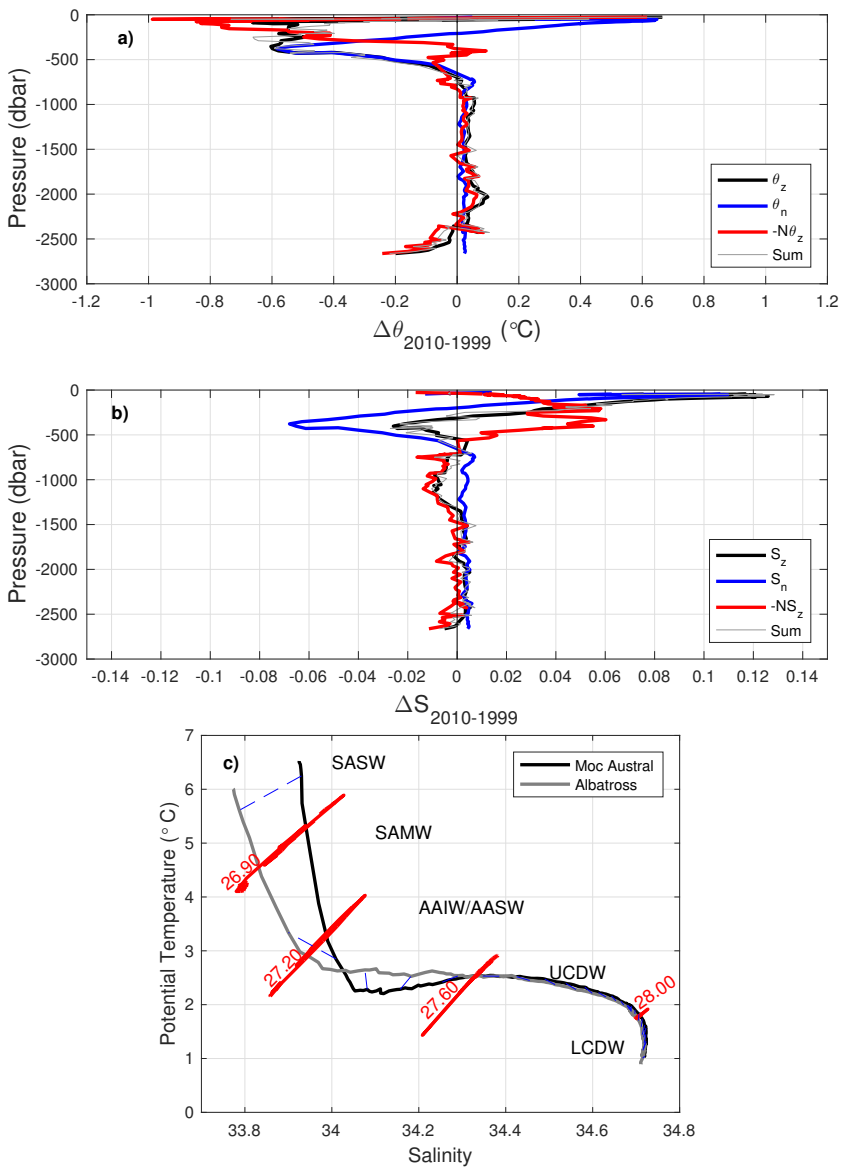

FIG. 5. Isobaric changes from 1999 to 2010 (θ_z, black line) decomposed into changes along neutral surfaces (θ_n, S_n,blue line) and changes due to the vertical displacement of isoneutrals (-Nθ_z, -NS_z red line) for (a) potential temperature and (b) salinity. The grey line shows the sum of both components. The lower panel (c) shows the average profile of θ/S for each cruise together with the densities that divide the water column into the different water masses (26.90, 27.20, 27.60 and 28.00 kg m^{-3}; red lines) and the link in between points of equal pressure (dashed blue lines).

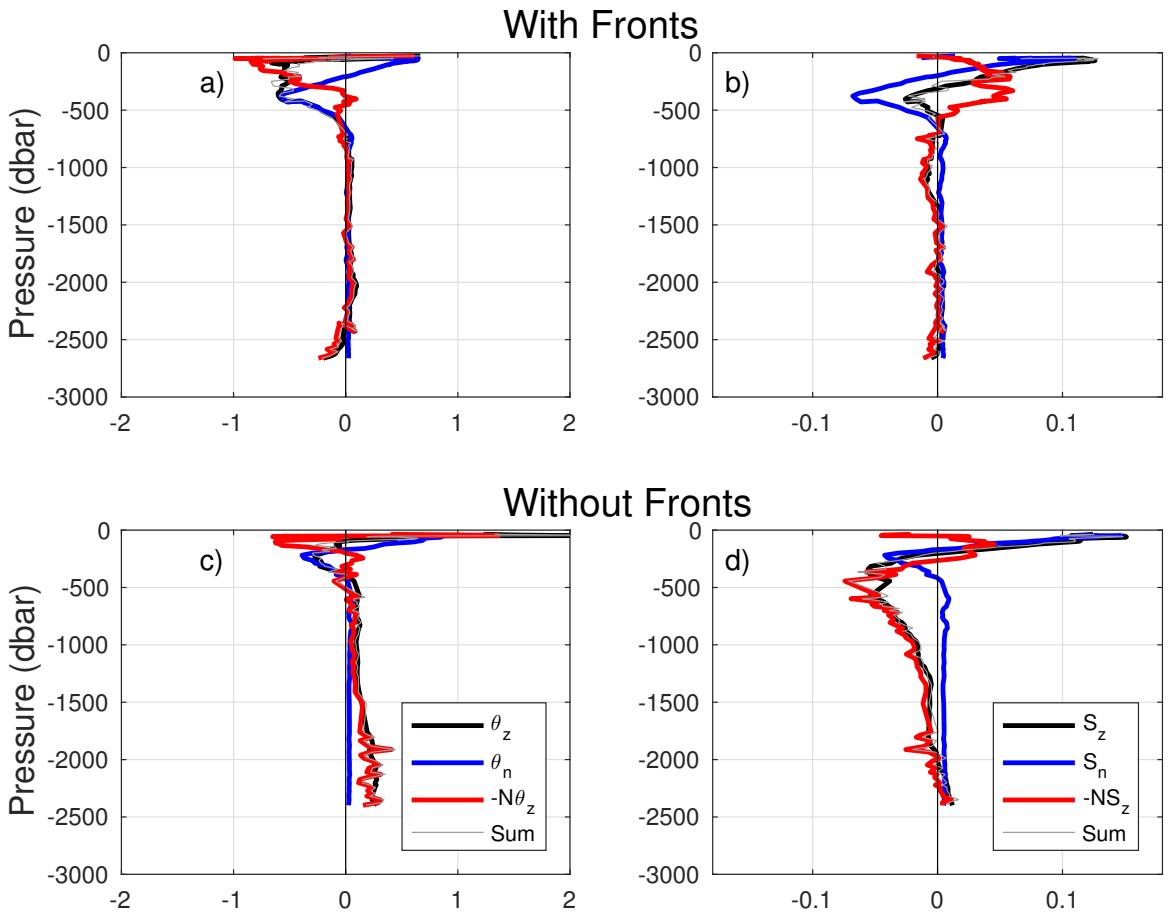

FIG. 6. Comparison between the isobaric changes from 1999 to 2010 carried out with the whole dataset of each year (a and b, same as Fig 5) and without the stations were the fronts are located (c and d). Isobaric changes from 1999 to 2010 (θ_z, black line) decomposed into changes along neutral surfaces (θ_n, Sn,blue line) and changes due to the vertical displacement of isoneutrals (-Nθ_z, -NS$_z$ red line) for temperature (a and c) and Salinity (b and d). The grey line shows the sum of both components.

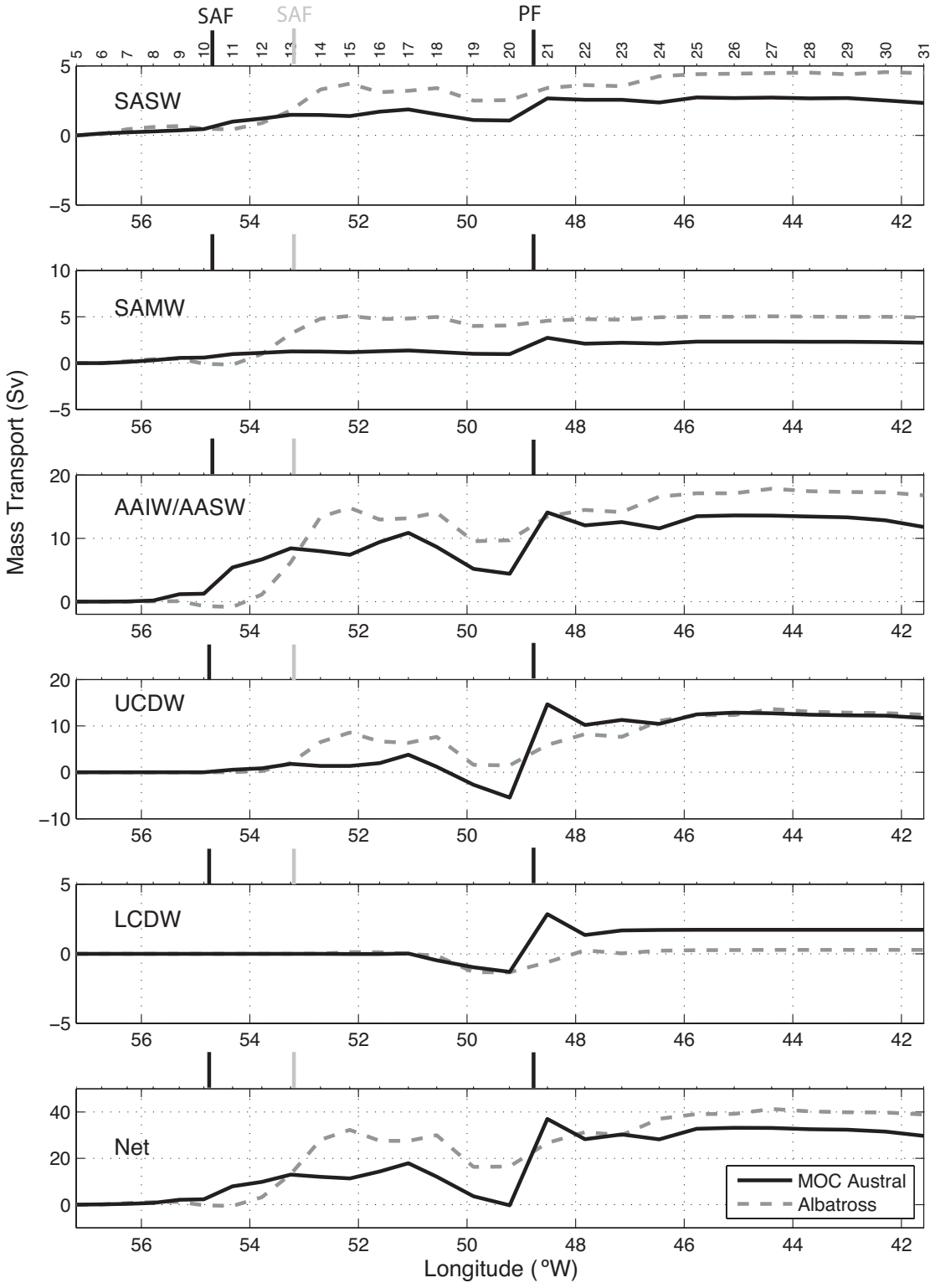

FIG. 7. West to east accumulated relative geostrophic mass transport, computed across the ALBATROSS and MOC-Austral hydrographic sections. Station numbering and the fronts (SAF and PF) location are displayed on top axis. Note the different vertical scales.

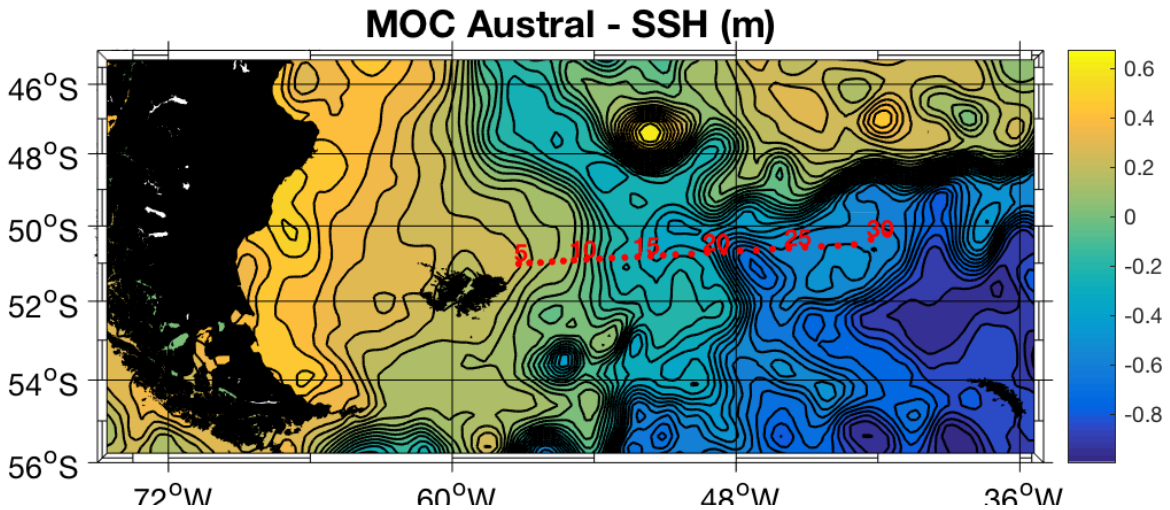

FIG. 8. AVISO Sea Surface Height (SSH) for the MOC-Austral cruise. Isolines have a separation of 5 cm.

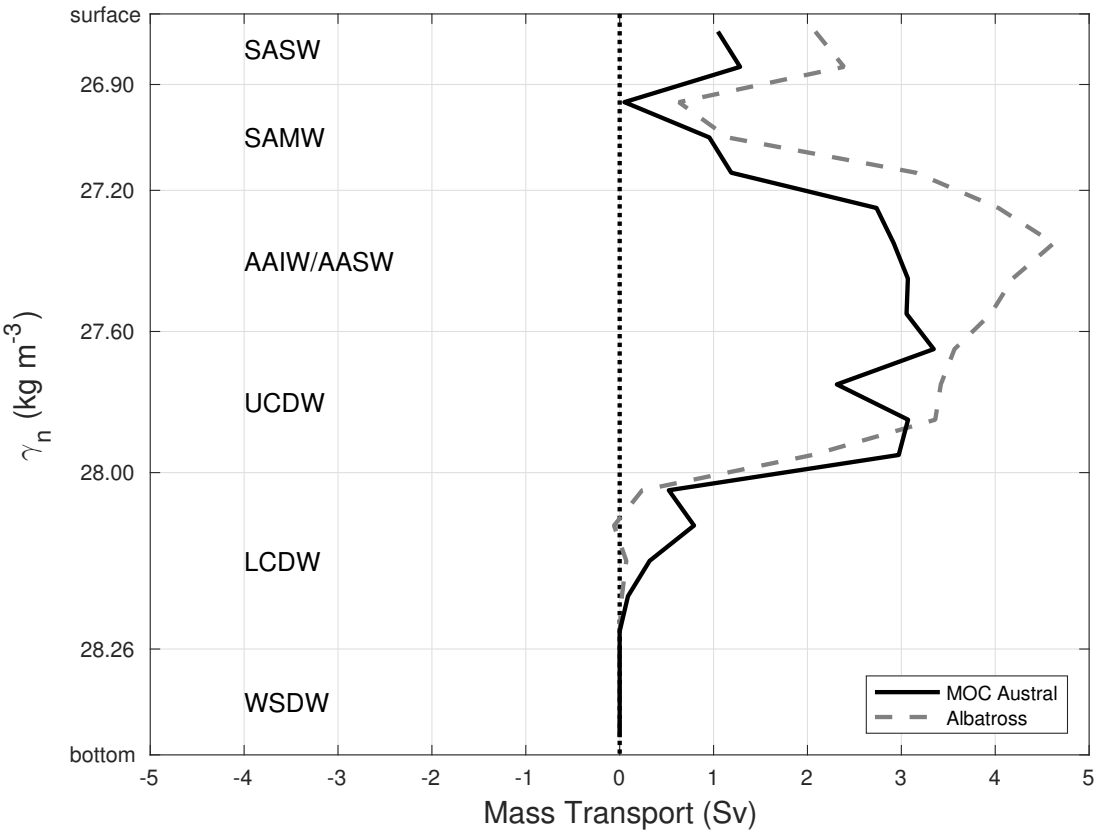

FIG. 9. Relative geostrophic mass transport per layer across the ALBATROSS and MOC-Austral sections.

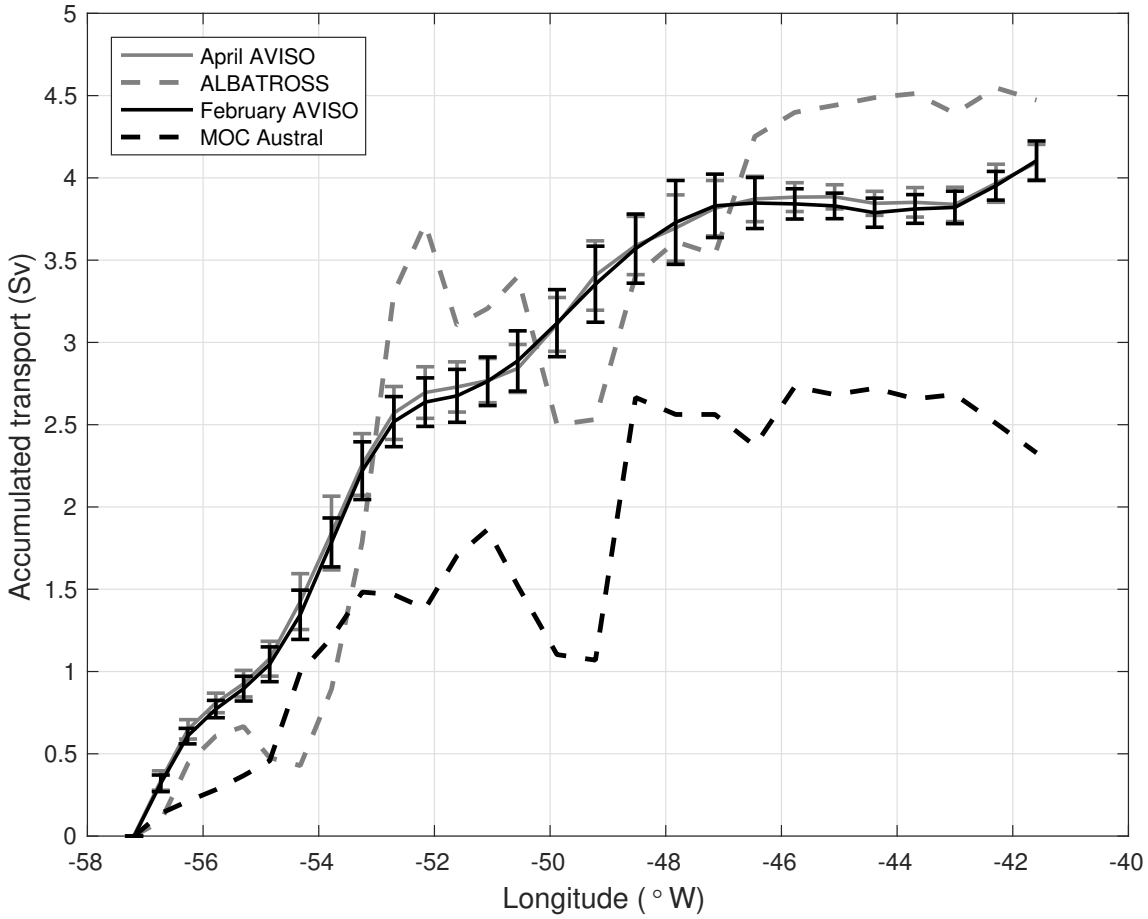

FIG. 10. West to East accumulated relative geostrophic mass transport from AVISO averaged from 1993 to 2016, together with their standard deviations: April (grey solid line) and February (black solid line). For this calculation, the depth of 50 m has been considered to compute the mass transport that corresponds to the SASW stratum. Dashed lines are the west to east accumulated relative geostrophic mass transports shown in Figure 7 for the SASW for the ALBATROS (grey) and MOC Austral (black) carried out in April and February, respectively.

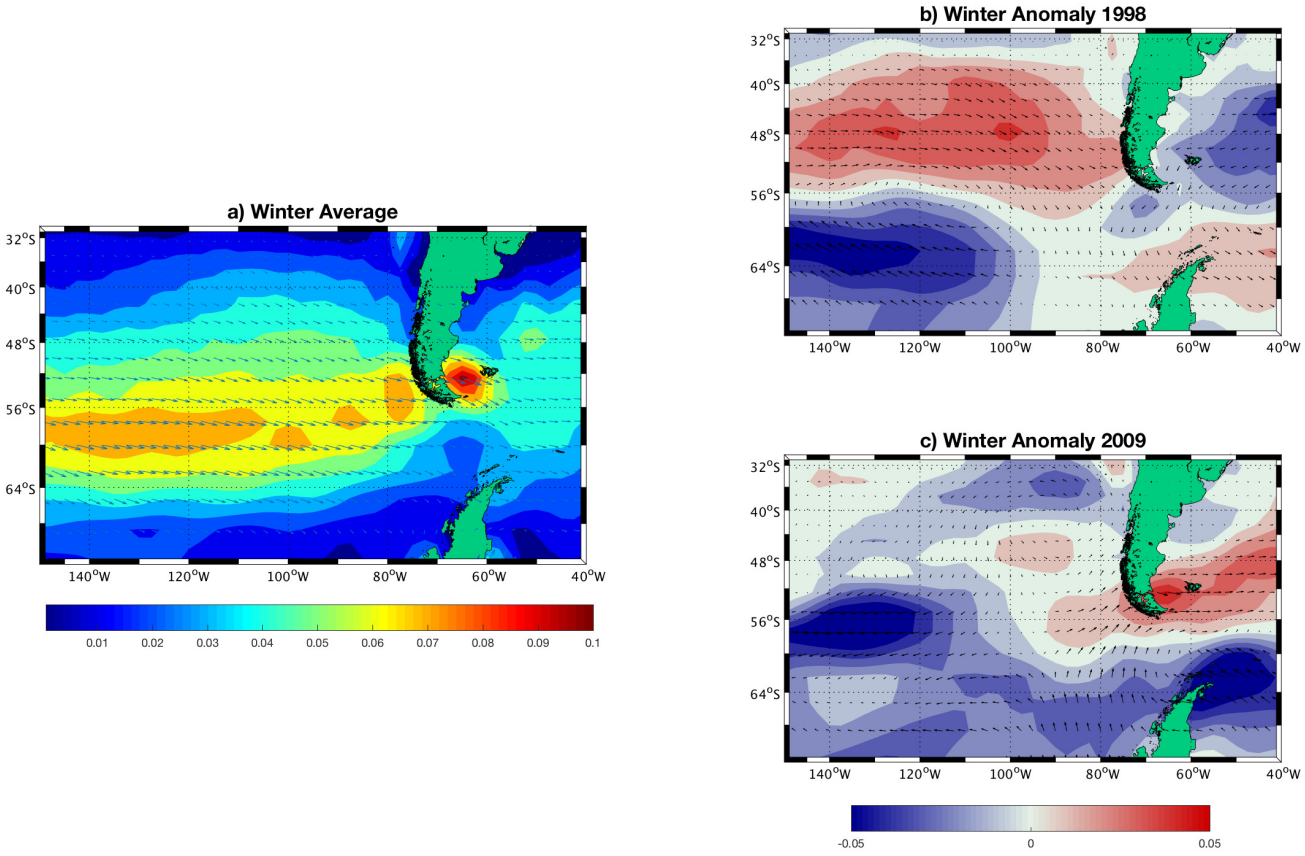

FIG. 11. Maps of NCEP-NCAR a) winter (July-September) mean wind stress in Pa (arrows, color indicates magnitude) for the time period 1998-2010. b) Winter wind stress anomaly (Pa) for year 1998. c) Same as b) but for 2009.